

Supporting Information

Crystal Structures and Optical Properties of New Quaternary Strontium Europium Aluminate Luminescent Nanoribbons

Xufan Li, John D. Budai, Feng Liu, Yu-Sheng Chen, Jane Y. Howe, Chengjun Sun,
Jonathan Z. Tischler, Richard S. Meltzer, Zhengwei Pan

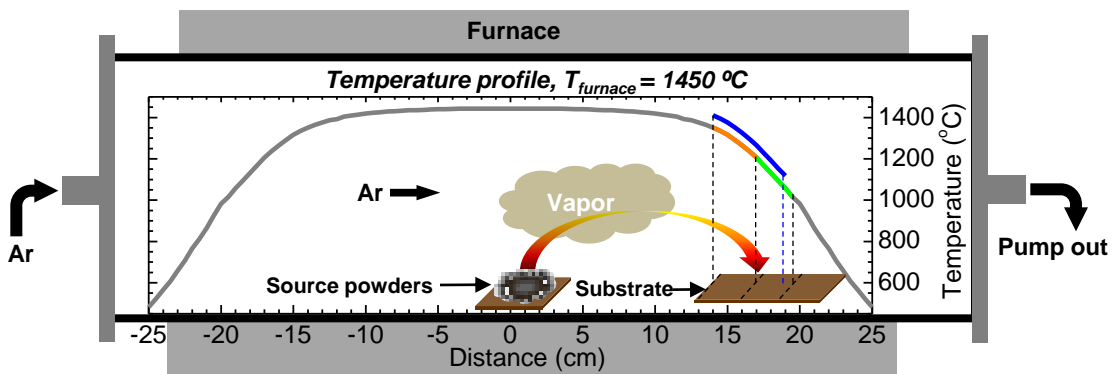


Figure S1. Schematic diagram of a tube furnace system. The grey curve represents the temperature profile along the alumina processing tube when the furnace temperature is set at 1450 $^{\circ}\text{C}$. The orange and green line segments along the temperature profile indicate the regions where the yellow- and green-luminescent SEAO nanoribbons are formed. The blue segment indicates the region where the blue-luminescent SEAO nanoribbons are formed. The blue segment is offset from the temperature profile for clarity.

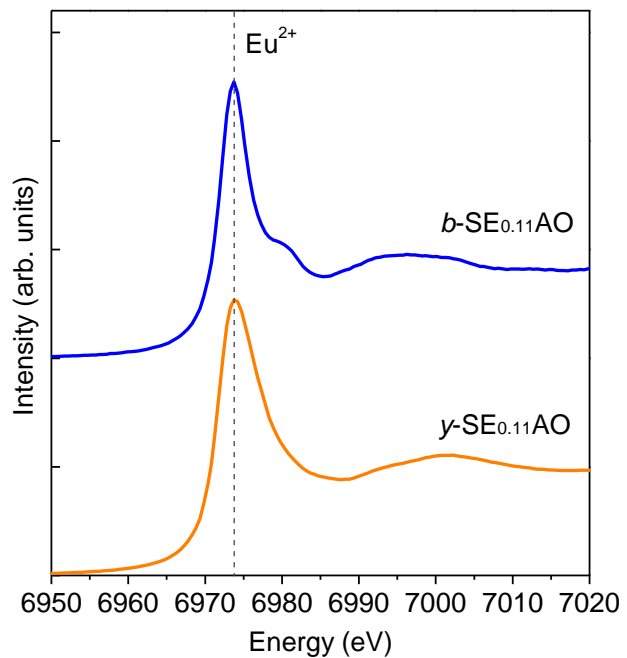


Figure S2. Eu L₃ x-ray near edge structure (XANES) spectra of *b*-SE_{0.11}AO and *y*-SE_{0.11}AO nanoribbons at room temperature. The resonance peaks at ~6974 eV are associated with Eu²⁺.

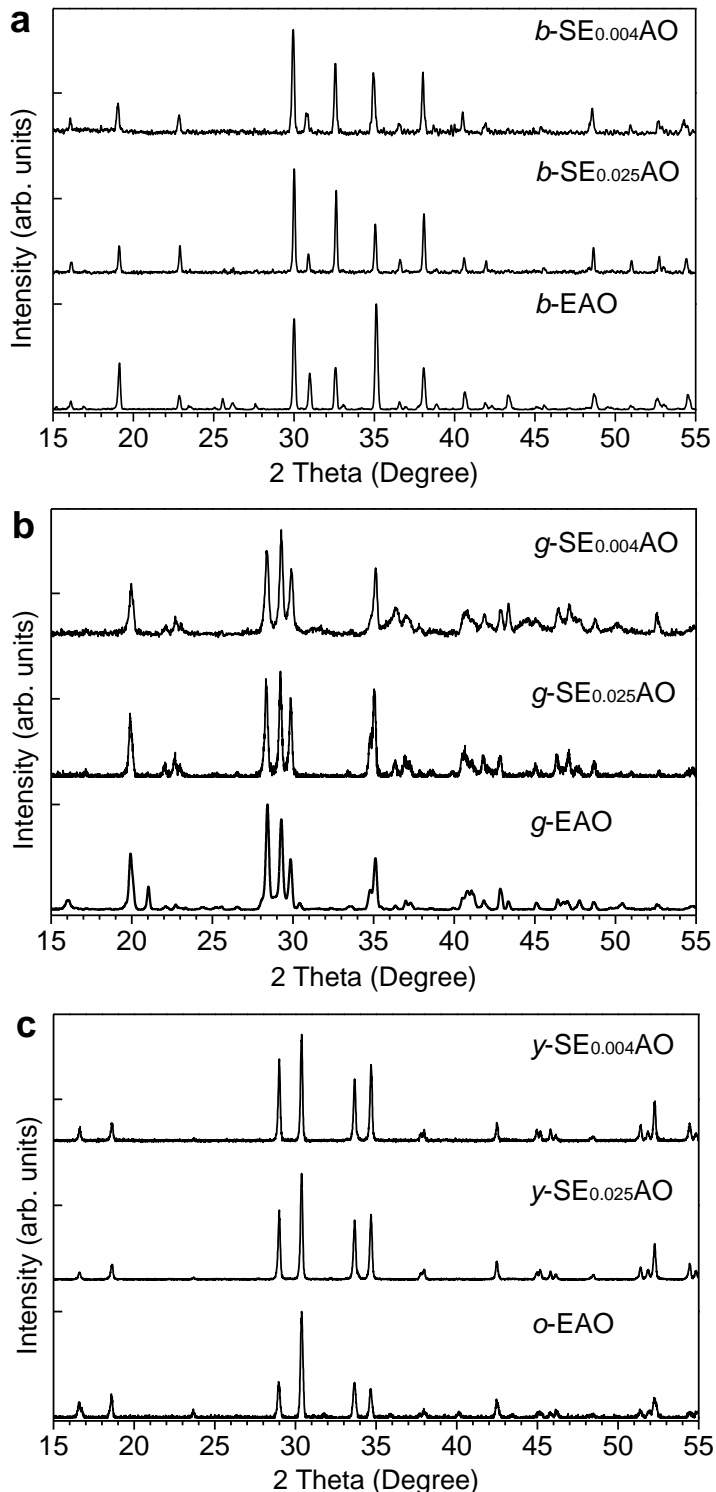


Figure S3. Conventional powder XRD patterns ($\lambda = 1.5406 \text{ \AA}$) of (a) $b\text{-SE}_{0.004}\text{AO}$, $b\text{-SE}_{0.025}\text{AO}$, and $b\text{-EAO}$, (b) $g\text{-SE}_{0.004}\text{AO}$, $g\text{-SE}_{0.025}\text{AO}$, and $g\text{-EAO}$, and (c) $y\text{-SE}_{0.004}\text{AO}$, $y\text{-SE}_{0.025}\text{AO}$, and $o\text{-EAO}$.

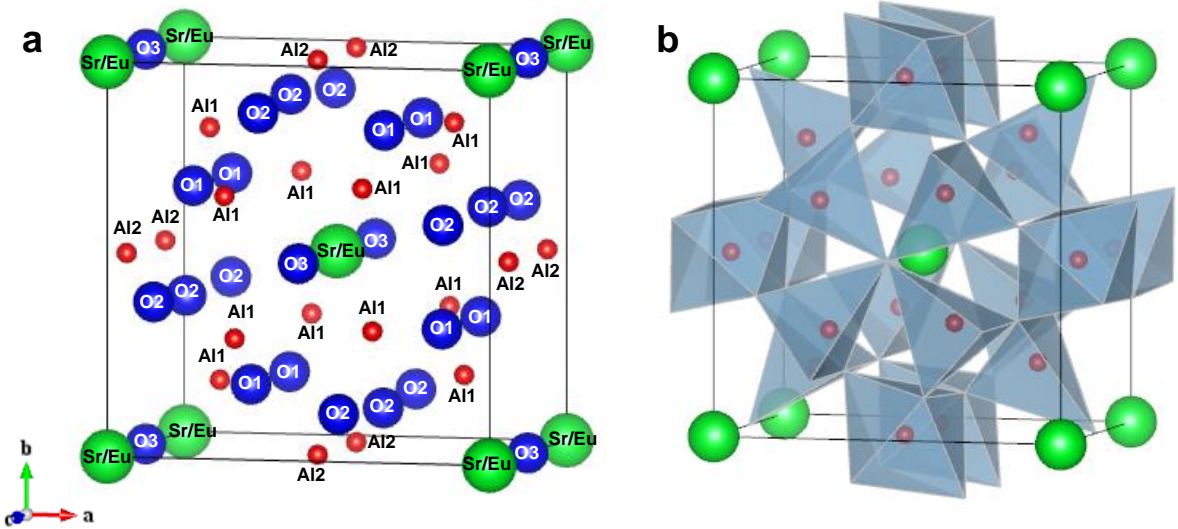


Figure S4. (a) Unit cell of $b\text{-SE}_{0.11}\text{AO}$ determined by synchrotron monochromatic microdiffraction using rotation crystallography at the APS 15-ID ChemMatCARS. Green balls: Sr/Eu atoms; red balls: Al atoms; blue balls: O atoms. See Table S4 for detailed atomic positions. (b) Unit cell of $b\text{-SE}_{0.11}\text{AO}$ showing AlO_6 octahedra and AlO_4 tetrahedra.

This unit cell and the atomic coordinates shown in Table S4 correspond to an R-factor least square fit of ~ 0.02 . The results show that $b\text{-SE}_{0.11}\text{AO}$ is based on a tetragonal unit cell with space group P4/mnc (#128) and lattice parameters of $a = b = 7.732 \text{ \AA}$ and $c = 5.837 \text{ \AA}$, which is in agreement with the results from JADE analysis. As shown in (a), the unit cell contains fully occupied 2 Sr/Eu (green balls), 8 A1 and 4 A2 sites (red balls), and 8 O1, 8 O2, and 2 O3 sites (blue balls) (see Table S4 for detailed atomic positions). The tetragonal structure of $b\text{-SE}_{0.11}\text{AO}$ is composed of alternating columns of AlO_6 octahedra and AlO_4 tetrahedra connected by sharing oxygen ions, and each Sr/Eu ion is surrounded by 12 O ions, with 2 at a distance of $\sim 2.92 \text{ \AA}$, 4 at $\sim 3.19 \text{ \AA}$, and 8 at $\sim 3.21 \text{ \AA}$, as illustrated in (b). Based on the unit cell presented in (a), the chemical composition for this structure is $(\text{SrEu})\text{Al}_6\text{O}_9$, with a net charge of +2, thus violating charge neutrality. To achieve charge balance, the structure most likely incorporates aluminum vacancies or oxygen interstitials. As described in the main text (see Figure 5), our observation of additional X-ray superlattice reflections in micro-Laue pattern shows that the tetragonal structure possesses a superstructure modulation along the c axis. This modulation typically has a periodicity close to three times the c -axis lattice parameter, and can be slightly incommensurate. We believe that the superstructure is associated with ordering of the Al vacancies or O interstitials across several of the smaller tetragonal unit cells in order to achieve charge balance. Thus far, our monochromatic X-ray crystallography data has not been able to measure the weak superstructure peaks from individual microcrystals. Additional synchrotron and electron microscopy studies aimed at characterizing the detailed nature of the superstructure order are continuing and will be reported in the future.

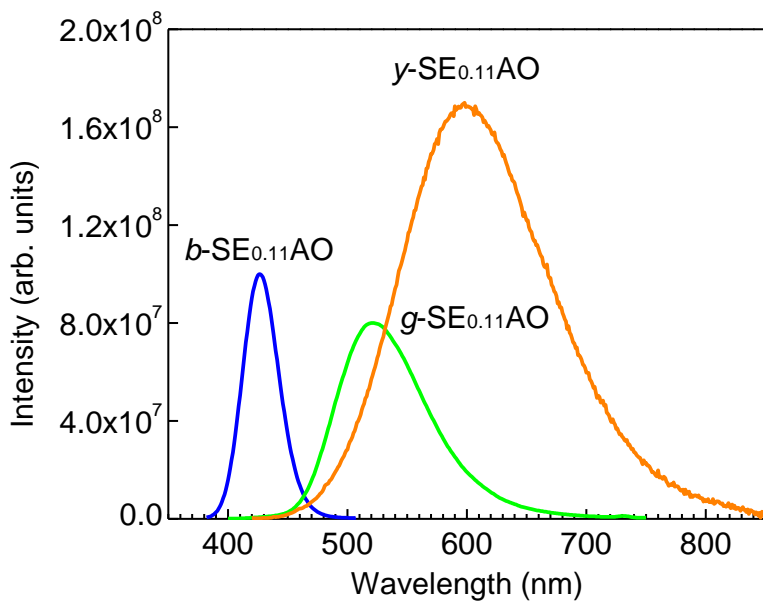


Figure S5. Non-normalized PL emission spectra of *b*-, *g*-, and *y*-SE_{0.11}AO nanoribbons under 360 nm excitation at room temperature.

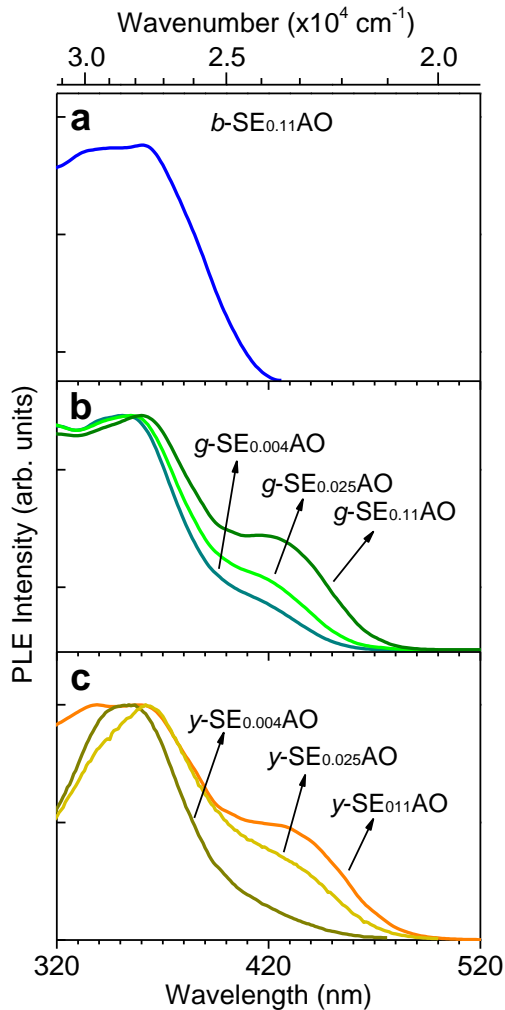


Figure S6. (a) PL excitation spectrum of *b*-SE_{0.11}AO monitoring at 420 nm emission at room temperature. (b) PL excitation spectrum of *g*-SE_{0.025}AO, and *g*-SE_{0.004}AO monitoring at 520 nm emission at room temperature. (c) PL excitation spectrum of *y*-SE_{0.11}AO, *y*-SE_{0.025}AO, and *y*-SE_{0.004}AO monitoring at 600 nm emission at room temperature. *b*-SEAOs with different Eu concentrations show the same excitation spectra as (a). The excitation spectra of *g*-SEAOs and *y*-SEAOs show shoulders at ~430 nm whose intensity decrease with the decrease of Eu concentration.

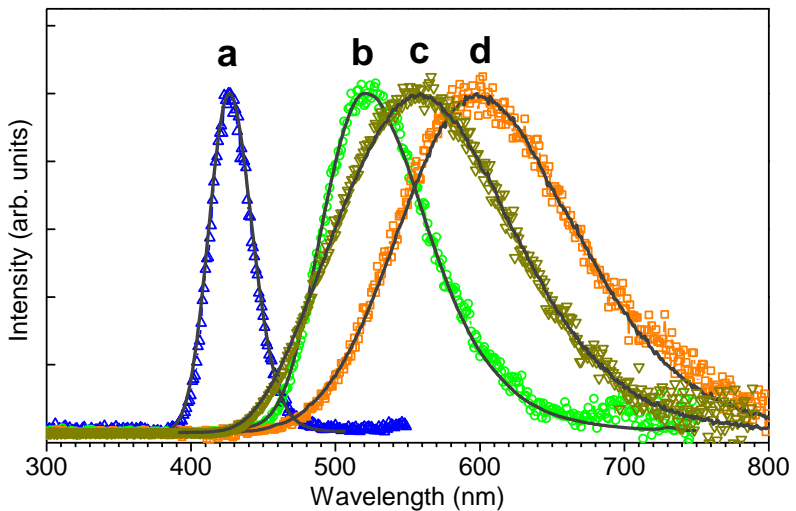


Figure S7. Emission spectra of (a) $b\text{-SE}_{0.025}\text{AO}$, (b) $g\text{-SE}_{0.025}\text{AO}$, (c) $y\text{-SE}_{0.004}\text{AO}$, and (d) $y\text{-SE}_{0.025}\text{AO}$ nanoribbons under the excitation of 360 nm UV light (solid curves) and synchrotron x-ray microbeam (scattered symbols) at room temperature. The spectra are normalized.

Table S1. Fitting information by JADE diffraction analysis software for the synchrotron powder XRD pattern of *b*-SE_{0.11}AO nanoribbons in Figure 4a.

a 7.754 Å	b 7.754 Å	c 5.803 Å	α 90°	β 90°	γ 90°			
2θ(obs.)	(h k l)	2θ(cal.)	Δ2θ	d(cal.)	d(obs.)	Δd	I%	
4.318	(1 1 0)	4.318	0.000	5.4833	5.4831	0.0002	15.7	
5.096	(1 0 1)	5.096	0.000	4.6462	4.6465	0.0002	25.4	
6.109	(2 0 0)	6.108	-0.001	3.8772	3.8766	0.0006	23.2	
6.830	(2 1 0)	6.830	0.000	3.4679	3.4677	0.0002	1.4	
7.959	(2 1 1)	7.958	-0.001	2.9768	2.9765	0.0004	100.0	
8.167	(0 0 2)	8.165	-0.002	2.9016	2.9008	0.0008	10.3	
8.642	(2 2 0)	8.642	0.000	2.7416	2.7416	0.0000	60.9	
9.240	(1 1 2)	9.240	0.000	2.5646	2.5646	0.0001	28.8	
9.665	(3 1 0)	9.665	0.000	2.4521	2.4520	0.0001	9.4	
10.038	(3 0 1)	10.038	0.000	2.3612	2.3611	0.0000	46.1	
10.204	(2 0 2)	10.203	-0.001	2.3231	2.3228	0.0002	2.7	
10.495	(3 1 1)	10.494	-0.001	2.2588	2.2586	0.0001	0.6	
10.654	(2 1 2)	10.652	-0.002	2.2253	2.2250	0.0004	7.6	
11.023	(3 2 0)	11.023	0.000	2.1507	2.1507	0.0000	5.8	
11.760	(3 2 1)	11.758	-0.001	2.0166	2.0164	0.0002	0.9	
11.900	(2 2 2)	11.900	0.000	1.9927	1.9927	0.0000	4.3	
12.234	(4 0 0)	12.234	0.000	1.9386	1.9385	0.0001	1.3	
12.612	(4 1 0)	12.612	0.000	1.8807	1.8806	0.0000	2.3	
12.666	(3 1 2)	12.664	-0.001	1.8729	1.8727	0.0002	15.1	
12.979	(3 3 0)	12.979	0.000	1.8277	1.8277	0.0000	1.3	
13.261	(4 1 1)	13.260	-0.001	1.7891	1.7890	0.0001	8.8	
13.684	(4 2 0)	13.684	0.000	1.7339	1.7339	0.0000	11.1	
13.733	(3 2 2)	13.733	0.000	1.7278	1.7278	0.0000	3.0	
14.050	(2 1 3)	14.047	-0.003	1.6893	1.6890	0.0003	7.1	
14.285	(4 2 1)	14.285	0.000	1.6613	1.6613	0.0000	0.5	
15.042	(4 1 2)	15.042	0.000	1.5782	1.5782	0.0000	0.7	
15.353	(3 3 2)	15.352	-0.001	1.5465	1.5464	0.0001	23.2	
15.615	(5 1 0)	15.614	-0.001	1.5207	1.5206	0.0001	1.7	
15.849	(5 0 1)	15.849	0.000	1.4983	1.4983	0.0000	1.8	
15.956	(4 2 2)	15.955	-0.001	1.4884	1.4883	0.0001	0.8	

Table S2. Fitting information by JADE diffraction analysis software for the synchrotron powder XRD pattern of y-SE_{0.11}AO nanoribbons in Figure 4b.

a 6.155 Å	b 6.155 Å	c 10.577 Å	α 90°	β 90°	γ 120°		
2θ(obs.)	(h k l)	2θ(cal.)	Δ2θ	d(cal.)	d(obs.)	Δd	I%
4.441	(1 0 0)	4.442	0.001	5.3300	5.3314	0.0014	9.5
4.476	(0 0 2)	4.477	0.001	5.2883	5.2896	0.0013	1.1
4.975	(1 0 1)	4.975	0.000	4.7598	4.7595	0.0003	22.7
6.308	(1 0 2)	6.309	0.000	3.7541	3.7544	0.0003	1.9
7.697	(1 1 0)	7.698	0.001	3.0773	3.0777	0.0003	34.3
8.057	(1 0 3)	8.057	0.000	2.9405	2.9404	0.0002	100.0
8.909	(1 1 2)	8.909	0.000	2.6598	2.6596	0.0001	40.3
8.962	(0 0 4)	8.961	-0.001	2.6442	2.6439	0.0003	1.8
9.169	(2 0 1)	9.169	0.000	2.5843	2.5844	0.0001	39.1
9.959	(2 0 2)	9.959	0.000	2.3799	2.3798	0.0001	4.3
10.006	(1 0 4)	10.006	0.000	2.3687	2.3687	0.0001	7.1
11.152	(2 0 3)	11.152	0.000	2.1260	2.1259	0.0001	13.6
11.771	(2 1 0)	11.770	-0.001	2.0146	2.0145	0.0001	2.9
11.824	(1 1 4)	11.824	0.000	2.0055	2.0055	0.0001	6.6
11.982	(2 1 1)	11.983	0.001	1.9790	1.9791	0.0001	3.6
12.061	(1 0 5)	12.061	0.000	1.9662	1.9662	0.0000	3.7
12.599	(2 1 2)	12.599	0.000	1.8826	1.8826	0.0000	1.0
12.637	(2 0 4)	12.636	-0.001	1.8771	1.8770	0.0001	3.1
13.352	(3 0 0)	13.353	0.001	1.7767	1.7768	0.0001	5.9
13.458	(0 0 6)	13.459	0.001	1.7628	1.7629	0.0001	5.8
13.564	(2 1 3)	13.564	0.000	1.7492	1.7492	0.0000	21.3
14.090	(3 0 2)	14.090	0.000	1.6842	1.6842	0.0000	8.0
14.179	(1 0 6)	14.179	0.000	1.6737	1.6737	0.0000	6.0
14.324	(2 0 5)	14.324	0.000	1.6569	1.6568	0.0000	11.9
14.814	(2 1 4)	14.813	-0.001	1.6025	1.6023	0.0002	2.4
15.431	(2 2 0)	15.431	0.000	1.5387	1.5386	0.0000	12.4
15.522	(1 1 6)	15.522	0.000	1.5296	1.5297	0.0000	4.4

Table S3. Atomic positions of $\gamma\text{-SE}_{0.11}\text{AO}$ determined by synchrotron monochromatic microdiffraction using rotation crystallography at the APS 15-ID ChemMatCARS facilities. The $\gamma\text{-SE}_{0.11}\text{AO}$ crystal has a hexagonal space lattice (Space group #163) with a set of lattice parameters of $a = b = 6.146 \text{ \AA}$, $c = 10.559 \text{ \AA}$, $\alpha = \beta = 90^\circ$, and $\gamma = 120^\circ$.

#	Atom	Label	Occupancy	X	y	z
1	Sr/Eu	Sr	1	0.667	0.333	0.919
2	Al	Al1	1	0	0	0
3	Al	Al2	1	0.164	0.327	0.750
4	O	O1	0.8	0.019	0.509	0.750
5	O	O2	0.4	0	0	0.8053
6	O	O3A	0.4	0.298	0.221	0.061
7	O	O3B	0.4	0.923	0.221	0.061

Table S4. Atomic positions of *b*-SE_{0.11}AO determined by synchrotron monochromatic microdiffraction using rotation crystallography at the APS 15-ID ChemMatCARS facilities. The *b*-SE_{0.11}AO crystal has a tetragonal space lattice (Space group #128) with lattice parameters of $a = b = 7.732 \text{ \AA}$ and $c = 5.837 \text{ \AA}$.

#	Atom	Label	Occupancy	x	y	z
1	Sr/Eu	Sr	1	0	0	0
2	Al	Al1	1	0.697	0.333	0
3	Al	Al2	1	0	0.500	0.250
4	O	O1	1	0.825	0.325	0.250
5	O	O2	1	0.605	0.121	0
6	O	O3	1	0.500	0.500	0